MNRAS **000**, 1–8 (2016) Preprint 10 November 2016 Compiled using MNRAS LATEX style file v3.0

Search For Type Ia Supernova NUV-Optical Subclasses

David Cinabro[1⋆], Daniel Scolnic[2,3], Richard Kessler[2,4], Ashley Li[2], and Jake Miller[1]
[1] *Wayne State University, Department of Physics and Astronomy, Deroit, MI, USA*
[2] *University of Chicago, Kavli Institute for Cosmological Physics, Chicago, IL, USA*
[3] *Hubble, KICP Fellow*
[4] *Department of Astronomy and Astrophysics, University of Chicago, Chicago, IL, USA*

arXiv:1611.02984v1 [astro-ph.CO] 9 Nov 2016

Accepted XXX. Received XXX; in original form XXX

ABSTRACT

In response to a recently reported observation of evidence for two classes of Type Ia Supernovae (SNe Ia) distinguished by their brightness in the rest-frame near ultraviolet (NUV), we search for the phenomenon in publicly available light-curve data. We use the SNANA supernova analysis package to simulate SN Ia-light curves in the Sloan Digital Sky Survey Supernova Search (SDSS) and the Supernova Legacy Survey (SNLS) with a model of two distinct ultraviolet classes of SNe Ia and a conventional model with a single broad distribution of SN-Ia ultraviolet brightnesses. We compare simulated distributions of rest-frame colors with these two models to those observed in 158 SNe Ia in the SDSS and SNLS data. The SNLS sample of 99 SNe Ia is in clearly better agreement with a model with one class of SN Ia light curves and shows no evidence for distinct NUV sub-classes. The SDSS sample of 59 SNe Ia with poorer color resolution does not distinguish between the two models.

Key words: stars: supernovae: general

1 INTRODUCTION

A recent claim in Milne et al. (2015) is that there are two distinct groups of Type Ia Supernovae (SNe Ia) distinguished by their brightness in rest frame near ultraviolet. The light curves of the two sets, red and blue, differ by 0.46 mag in their $u-v$ colors at the time of peak brightness in the rest-frame B band (B-peak) where the color is derived from spectrophotometry of 23 SNe Ia observed with the UVOT instrument on the SWIFT satellite (Roming et al. 2005) and 52 SNe Ia observed with Keck and the VLT with spectrophotometry matched to the UVOT system. The two sets have a 0.34 mag difference in the $u-b$ color and an insignificant difference in the $b-v$ color at peak brightness. Further, the fractions of SN Ia in the red and blue sets change as a function of redshift with the red sample dominant (60-70% of the total) at redshifts smaller than 0.1, and the blue sample dominant (80-90% of the total) at redshifts from 0.4 to 1.0. The study also found SNe Ia in the red sample exhibited larger ejecta velocities in their spectral features. Milne et al. (2015) claims that SNe Ia light curve fits for the red sample will underestimate the host galaxy extinction, leading to a redshift dependent bias in the corrected peak brightness and also in the inferred cosmological parameters.

The importance of SNe Ia in modern cosmology cannot be understated. Observations just before the turn of the century provided the first clear evidence of an accelerated expansion of the universe (Riess et al. 1998; Perlmutter et al. 1999) and subsequent observations combined with the clustering of galaxies and the cosmic microwave background point towards this acceleration being caused by a negative pressure fluid, dubbed Dark Energy (Olive et al. 2014). These observations and the precision of the extraction of cosmological parameters inferred from SNe Ia depend on the assumption that the light curves of SNe Ia at low redshift are standardized in the same way as SNe Ia at high redshift. The observations of Milne et al. (2015) call this underpinning assumption into question.

The modeling of the rest frame ultraviolet brightnesses of SNe Ia is more difficult than in the visible. SNe Ia are dimmer in the rest frame ultraviolet than the visible, the effects of extinction are larger in the ultraviolet, and ground based observations are difficult with large and highly variable ultraviolet atmospheric absorption. The Joint Lightcurve Analysis (Betoule et al. 2014) (JLA) is the largest sample to date used for SN Ia cosmology, and they have publicly released many high quality SN Ia light curves. In the JLA, the ultraviolet behavior of SN Ia is empirically modeled with a distribution of brightnesses that is much broader than the distribution in the visible. This model does not agree with the Milne et al. (2015) observation of two narrow and distinct distributions in the ultraviolet.

Checking the claim of Milne et al. (2015) with the JLA data is not as simple as it might seem. At low redshift,

⋆ E-mail: david.cinabro@wayne.edu

© 2016 The Authors

the JLA sample is made of a heterogeneous collection of SN Ia light curves observed by many different instruments and surveys. Unknown selection effects for this sub-sample make it difficult to interpret (Scolnic et al. 2014). To avoid possible biases from selection effects, we use the SDSS-II (Frieman et al. 2008) and SNLS (Astier et al. 2006) SN Ia samples, whose selection effects are well modeled with Monte Carlo simulations (Kessler et al. 2013; Betoule et al. 2014). However, these samples are not well suited to ultraviolet photometry. The SDSS $u-$filter is less efficient than the $g-$, $r-$, $i-$filters, and the survey found only 12 securely identified SNe Ia at redshift smaller below 0.1 which could be used to directly check the Milne et al. (2015) observation. The SNLS data does not provide ultraviolet filter photometry. With insufficient ultraviolet SN Ia data in the public domain, a more promising approach is to look at higher redshift where the rest frame ultraviolet is observed in the visible. From redshift of 0.3 to 0.7, the spectral range of the rest frame UVOT $u-$, $v-$, and $b-$filters is observed in the SDSS and SNLS $g-$, $r-$, and $i-$filters.

The next section describes the models of SN Ia light curves that we used to check the observations in Milne et al. (2015). Section 3 describes our simulations of the SDSS-II and SNLS surveys, and the predictions based on our model of the Milne et al. (2015) observation. In Section 4 we compare the observed SN Ia light curves with the two models, and we end with a short conclusion.

2 SN IA MODELS

We use the publicly available SNANA (Kessler et al. 2009)[1] package to perform the analysis described below. SNANA is a supernova light curve analysis package that allows for detailed simulations of SNIa light curves for arbitrary instruments, cadences and observing conditions. To develop a model for the Milne et al. (2015) observations, we simulate SNIa light curves with infinite photon statistics observed with an error free instrument at redshift of 0.01, called "perfect mode", to view and compare rest-frame models without instrumental effects. We observe the time dependence of the colors and B-peak colors in the filters on the UVOT instrument (Breeveld et al. 2011). Our goal here is to develop a SN Ia light curve model that reproduces the Milne observations and compare it to an existing, more conventional description of SNe Ia ultraviolet brightness.

We simulate light curves in the UVOT passbands to compare with Milne et al. (2015), and also in the SDSS and SNLS passbands, as described in the JLA (Betoule et al. 2014), to compare with data. The filters of the SDSS and SNLS are similar, but not exactly the same. Table 1 gives the central wavelengths of the filters we reference in this work.

Our base model for SN Ia light curves is the SALT-II model (Guy et al. 2010). The model describes the shape of light curves with two parameters, x_1, which gives the width-luminosity relation, and c, the color parameter which parametrizes intrinsic SN Ia colors and the effect of extinction. The parent population of these parameters used in our conventional simulation follow those measured by Scolnic and Kessler (Scolnic & Kessler 2016), and thus we call this the SK16 model. Figure 1 shows the time dependence of the rest frame colors in the UVOT filters and within one day of B-peak in this SK16 model. The model includes the effect of Milky Way extinction from Schlegel et al. (1998). The observed scatter is due to a combination of intrinsic brightness variations, the underlying population of color (c) and stretch (x_1), and Milky Way extinction. In this model the ultraviolet part of the spectrum shows a larger scatter than in the visible.

[1] http://snana.uchicago.edu

Table 1. Central wavelengths of the filters used in this work. Details of the UVOT filters can be found in Breeveld et al. (2011) and for the SDSS and SNLS filters in Betoule et al. (2014).

The UVOT filters are similar to the standard Bessel filters.

Name	Central Wavelength (Å)
UVOT-u	3465
UVOT-b	4392
UVOT-v	5468
SDSS/SNLS-g	4760
SDSS/SNLS-r	6230
SDSS/SNLS-i	7630
SDSS/SNLS-z	9130

We develop a model of the Milne et al. (2015) observation by introducing two classes of light curves distinguished by their brightnesses in the ultraviolet part of the spectrum. The resolution of the UVOT photometry, the red and blue histograms in Figure 2 of Milne et al. (2015) showing the $u-v$-color for example, is between 0.05 and 0.07 mag (Milne 2016). Given the observed width of the two color peaks, in the range of 0.07-0.09 mag, this implies the contribution to the width due to the properties of the observed SN Ia (the stretch distribution and Milky Way extinction) is very narrow, less than 0.05 mag.

To reproduce the observed features we modify the base prediction of the SALT-II rest frame spectral flux, F, in the wavelength range 2700 Å to 4300 Å by

$$F = F^{(-0.4\mathrm{dm})}, \quad (1)$$

where

$$\mathrm{dm} = \pm\left(\frac{0.55}{2}\right)\sin\left(\pi\frac{(\lambda - 2700\text{Å})}{1600\text{Å}}\right)(1+0.04\mathrm{R_G})\mathrm{mag}. \quad (2)$$

The wavelength, λ, is in Angstroms, and $\mathrm{R_G}$ is a Gaussian distributed random number with standard deviation of one. The amplitude and wavelength range of this bifurcation is chosen to match the color separations in Milne et al. (2015). The amplitude is larger than the observed $u-v$ color separation as it represents the maximum separation at only one wavelength, while the color comes from integrating over the wavelength range of the $u-$filter. The size of the Gaussian smearing reproduces the narrow width of the NUV peaks. Over the entire wavelength range there is an additional coherent scatter drawn from a Gaussian with a width 0.08 mag matching the width of the SNe Ia brightness distribution. Those light curves with the brighter ultraviolet distortion are the "blue" sample and those with the dimmer are the "red" sample, and a random selection between the two is made for each light curve.

We find that Equations 1 and 2 combined with non-zero values for the SALT-II c parameter results in $u-v$

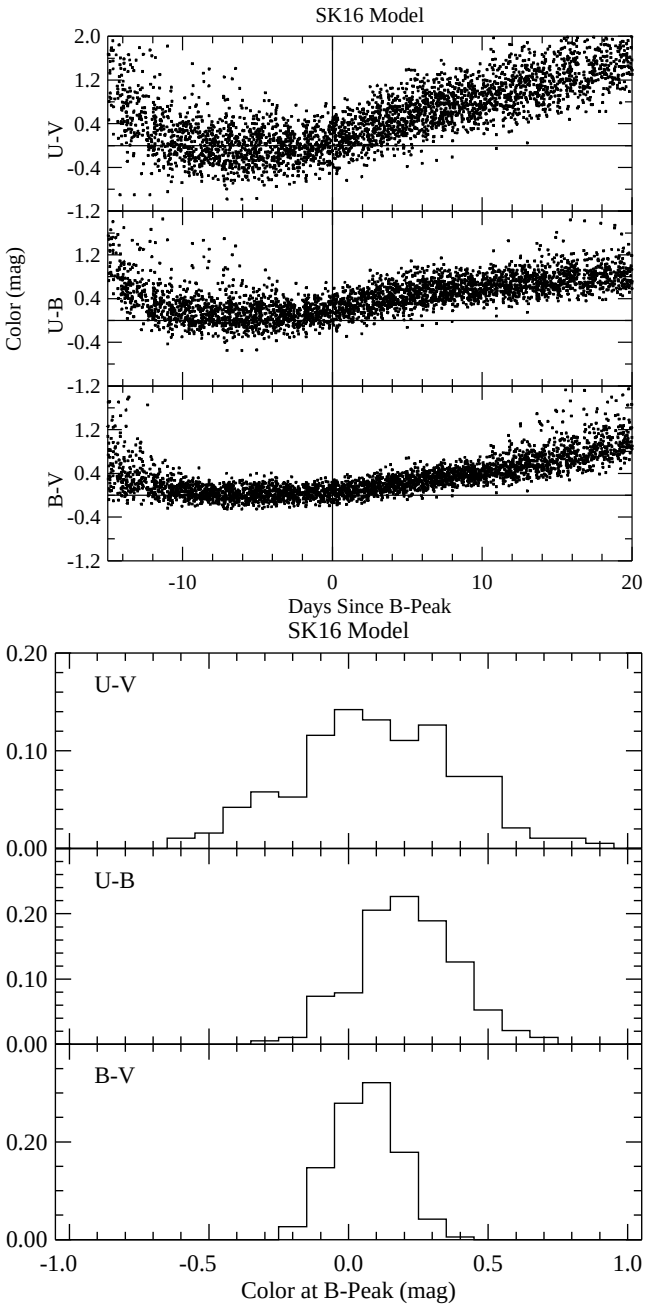

Figure 1. Rest frame colors in the UVOT filters for the SK16 model in SNANA perfect mode as described in the text of SN Ia versus the time since the B-peak (top) and within one day of the B-peak (bottom).

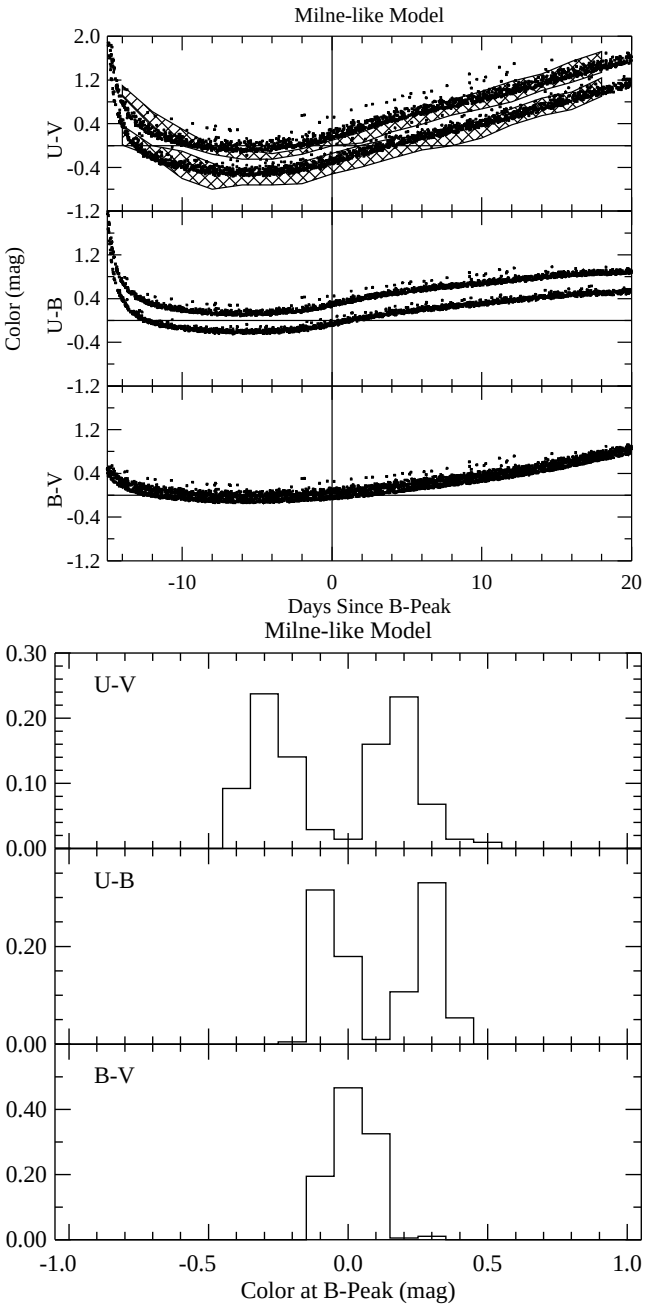

Figure 2. Using the SNANA "perfect mode" simulation for the Milne-like model, the top panel shows UVOT rest-frame colors versus time, and the bottom panel shows rest-frame colors within one day of B-peak. In the topmost panel showing the $u-v$-color versus time, the hatched regions are the range of red, upper, and blue, lower, sample colors taken from Figure 1 of Milne et al. (2015).

color peaks that are too broad to be consistent with the Milne et al. (2015) observation. To preserve the sharp color features, we set the SALT-II color parameter, c, to zero. With $c = 0$, Figure 2 shows time dependence of the rest frame colors in the UVOT filters and the colors within one day of B-peak in this "Milne-like" model. At B-peak, the width and separation of the red and blue peaks in the $u-v$ and $u-b$ colors agrees well with Milne et al. (2015). The population of the two classes is equal in these illustrations. This model reproduces well the data displayed in Figures 1-3, 9-12, and Table 2 in Milne et al. (2015). It also incorporates the same variations of the SALT-II x_1 parameter and expected Milky Way extinction as we use in the SK16 model described above.

In the Milne-like model, variation in an extracted value of the SALT-II color parameter away from zero is caused by the two different classes of SNe Ia in the ultraviolet, red and blue, rather than an underlying intrinsic color population as described in Scolnic & Kessler (2016). Other choices for the parameters of the bifurcation given in 2 such as narrowing

the wavelength range to 2700-3700 Å or reducing the magnitude of the separation are discussed further in Section 4.

3 SIMULATION OF SN IA SURVEYS

Using the SK16 and Milne-like models, we simulate SN Ia light curves corresponding to the SDSS and SNLS data in the JLA. Our goal here is to use the JLA data to compare against the two models when all observational effects are included, and develop a method of choosing between the two models. The simulations of the SDSS and SNLS supernova surveys include the exact cadence of observations, photometric uncertainties, redshift distributions, and spectroscopic identification efficiencies observed in the surveys.

To ensure robust light curve fits, we apply selection requirements to both the data and simulation. We require at least five epochs of observation in at least three of the $g-$, $r-$, $i-$, and $z-$bands. Observations must have a flux measured with signal to noise better than 3.0 in g, r, i and 1.0 in z. Light curves passing these criteria are fit with the SALT-II model. We only consider epochs within -15 and $+50$ days of the fitted B-peak in the rest frame. The results of the fit are accepted if there is at least one epoch before and three after the B-peak, and the fit has a χ^2 probability of greater than 0.001. We simulate samples that are about 15 times larger than the data samples. We consider SN Ia with redshifts in the range 0.3 to 0.4 for the SDSS and 0.3 to 0.7 for the SNLS.

These selections mirror the requirements on the JLA sample except that we require the presence of z-band photometry. The simulation predicts that 9% of SNe Ia light curves in the JLA sample in the indicated redshift ranges will not pass to our sample.

We extract the rest frame colors using the fitting procedure described in Section 4.3 of Kessler et al. (2013). Briefly, after an initial fit to the SALT-II model, additional constrained fits are done to the photometry results of the two observer frame filters that most closely correspond to the best match in redshifted wavelength to the desired rest frame filter photometry. The procedure introduces a negligible additional uncertainty on the rest frame colors, and allows direct comparisons between the photometric observations of SDSS and SNLS with the spectrophotometric observations in Milne et al. (2015). Figure 3 shows the distribution of colors at B-peak we expect from the two surveys for the two models.

The analysis of simulated SNe Ia shows that we could clearly distinguish between the Milne-like model, with two peaks clearly seen in the distribution of the $u-v$ color, and the SK16 model, with the $u-v$ color distribution appearing as one broad peak, in the SNLS survey. In the SDSS survey it is more difficult to see a difference with only a hint of two peaks for the Milne-like model, but the SK16 model produces a slightly narrower distribution of the $u-v$ and $u-b$ colors than the SK16 model. The resolution of the B-peak colors of the SNLS is better than the SDSS.

Further, we note that the fitted SALT-II color parameter is also sensitive to the two models. Figure 4 shows the distribution of the fitted value for c in the two simulated surveys for the two models. There is a clear difference between the two models. The SNLS simulation shows two narrow peaks for the Milne-like model and one broad peak for the SK16 model. The simulation of the SDSS shows a broader distribution for the Milne-like model than the SK16 model. The distribution of the fitted value of c is sensitive to the different predictions of the two models.

We note that the rest frame colors are highly correlated with the fitted value of c and considering only one of the distributions, c or $u-v$ color for example, is sufficient to discriminate between the SK16 and Milne-like models for the brightness of SNe Ia in the rest frame ultraviolet.

4 COMPARISON OF SURVEY OBSERVATIONS AND SIMULATIONS

We apply the analysis described above to the data from the SDSS and SNLS supernova surveys in the JLA sample. This only includes light curves that have been clearly typed with spectroscopy as SN Ia, and thus their redshifts are well measured. Our analysis accepts 59 and 99 light curves in the SDSS and SNLS respectively. After applying our redshift cuts to the JLA sample, the other cuts reject 9 light curves ($5 \pm 2\%$), consistent with the simulation prediction or 9%.

The redshift distributions for the SN Ia light curves accepted for analysis by both surveys agree well with the simulation showing that efficiency and selection effects are well modeled. The distributions for the SALT-II x_1 parameter and the uncertainty on the peak time also agree well between the simulation and the data showing that the results of the SALT-II fits to the accepted light curves are also well modeled by the simulation. The uncertainty on the peak time also contributes to the resolution of B-peak colors. The simulated results for both the SK16 model and Milne-like model in these parameters show no obvious dependence on the two underlying SN Ia light curve models. Figures 5 and 6 compare the results of our simulations with the results of the data analysis for these parameters.

Figure 7 compares the distribution of the fitted rest frame colors among the SNLS and SDSS data with simulations of the SK16 and Milne-like models. Here the Milne-like model has 50% red and 50% blue light curves. The colors at B-peak clearly agree better with the SK16 model showing a wide distribution in $u-v$ rather than two narrow peaks in the SNLS as we would expect in the Milne-like model. For the SDSS, the $u-v$ distribution is slightly narrower compared to the Milne-like model. The comparison is less clear for the $u-b$ color where the Milne-like model distribution is wider than the data, and the difference between the SK16 and Milne-like models is smaller. There is no obvious difference between the data and the two models in the $b-v$ color.

Figure 8 compares the distribution of the fitted SALT-II color parameter between the data and the simulations. We considered three models of this distribution to compare with the data in a simple χ^2 minimization. The first model is SK16, and it is fit to the data with fixed shape allowing only the distribution's area to vary. The second is the Milne-like model where the predictions for the fractions of blue and red light curves are taken from the observations displayed in Figure 4 of (Milne et al. 2015): roughly 70% and 30% respectively in the SDSS corresponding to the redshift range of 0.3-0.4 and 80% and 20% in the SNLS in the redshift range

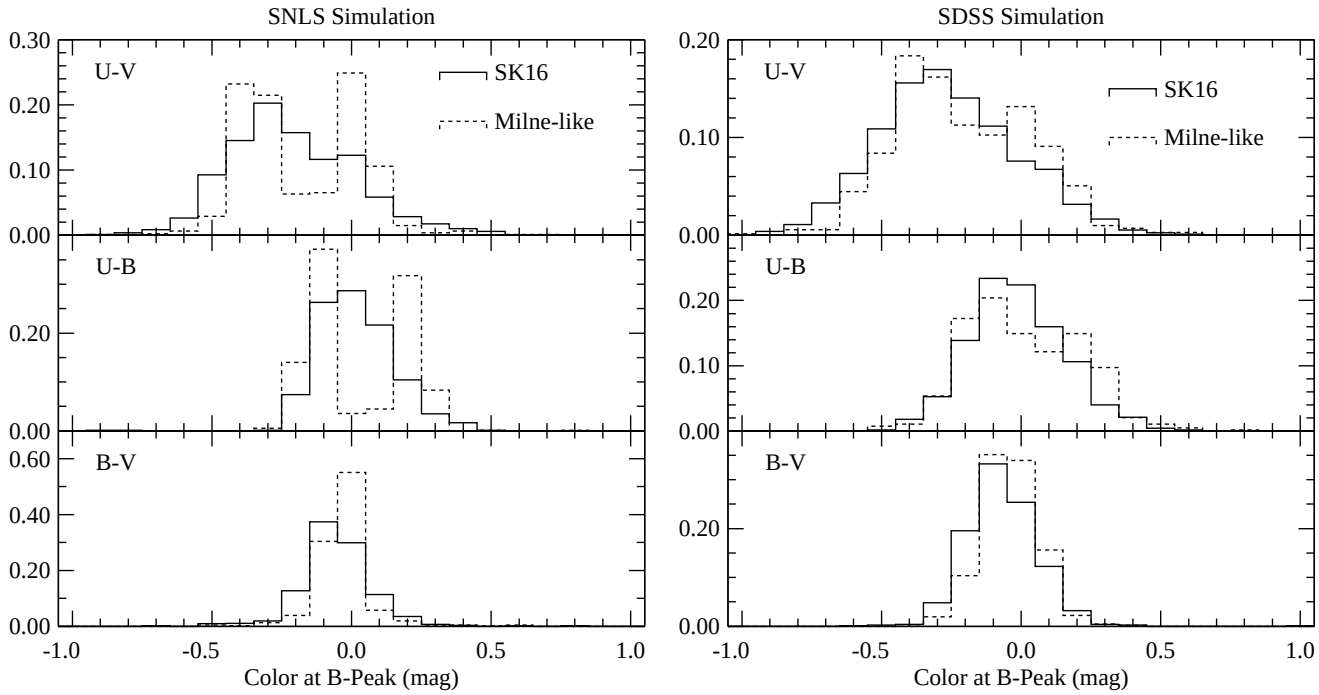

Figure 3. The fitted values of the restframe colors at B-peak for the SK16 and Milne-like models as described in the text for simulations of the SNLS (left) and SDSS (right) surveys.

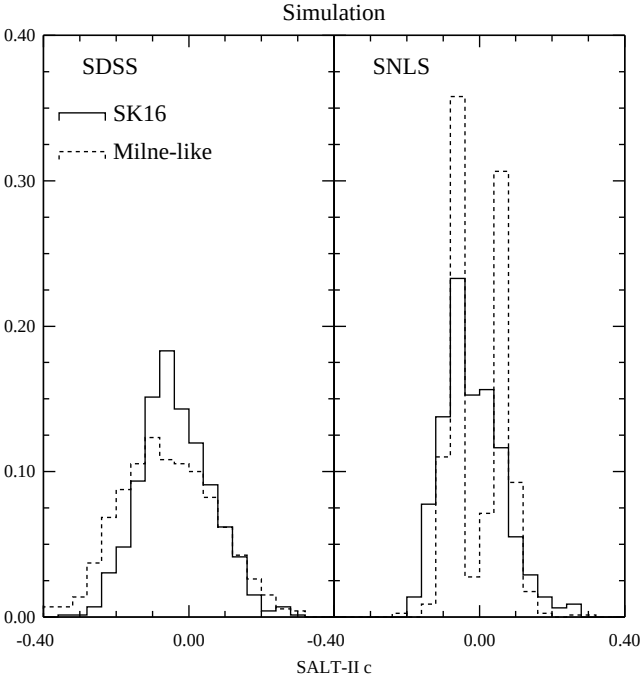

Figure 4. For simulations of the SK16 (solid) and Milne-like (dashed) models, the fitted SALT-II color parameter (c) is shown for SDSS (left) and SNLS (right).

0.3-0.7. We also fit this model to the data only allowing its area to vary. The third is a variant of the Milne-like model where we allow the areas of the contributions from the red and blue distributions to vary independently.

In the SNLS data the SK16 model is decisively favored. As can be seen on the right of Figure 8, this model, the solid histogram, agrees reasonably well with the data, dots, and gives $\chi^2 = 18$ for 8 degrees of freedom. Note that we did no tuning of the parameters of this model to match our data set, but simply used the parameters found in a very different analysis done by Scolnic and Kessler (Scolnic & Kessler 2016). The Milne-like model with fixed fractions of blue and red light curves fits poorly giving $\chi^2 = 49$. The Milne-like model with floating fractions of blue and red light curves also agrees poorly with the data giving $\chi^2 = 47$ for 7 degrees of freedom. This fit has $(41 \pm 10)\%$ of the light curves from the blue sample, and is displayed as the dashed histogram in the right panel of Figure 8. The relative probability of the Milne-like model based on the χ^2 probability for these fits is smaller than 3×10^{-6}.

The results for the SDSS data, left side of Figure 8, are not able to distinguish between the two models. The fit to the SK16 model agrees well, giving a $\chi^2 = 7$ for 9 degrees of freedom and is shown by the solid histogram. The fits to the Milne-like model with fixed blue and red light curve fractions gives $\chi^2 = 12$, and the Milne-like model with floating light curve fractions gives $\chi^2 = 12$ for 8 degrees of freedom with $(49 \pm 16)\%$ blue light curves. This latter fit is shown by the dashed histogram. That the SDSS data has poorer discrimination power than the SNLS data is not surprising given the smaller number of SN Ia in the SDSS sample and poorer resolution on the peak colors than the SNLS. Nevertheless the SDSS data show excellent agreement with the SK16 model.

We explore variations of the Milne-like model consistent with the Milne et al. (2015) observation including details of the bifurcation in the ultraviolet and the size of the color separation. We reduced the wavelength range of the bifurcation between the red and blue sample from 2700–4300 Å to 2700–3700 Å and varied the $u-v$ red and blue color separa-

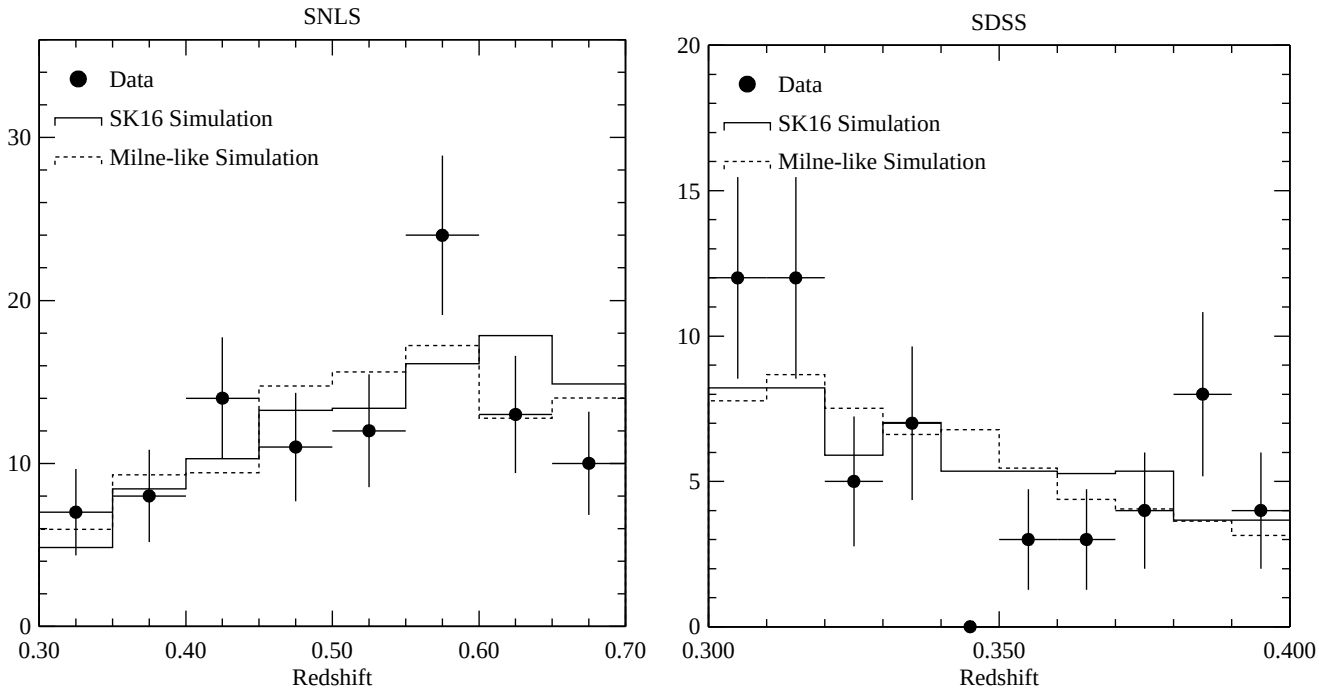

Figure 5. The Redshift distribution of the SN Ia accepted in the analysis comparing the data and simulations of the SK16 and Milne-like models as described in the text in the SNLS (left) and SDSS (right) surveys.

tion in the range of 0.26-0.55 mag from the central 0.46 mag. Those with a smaller color separation agreed better with the SNLS data, but never having a χ^2 probability relative to the SK16 model larger than 4×10^{-5}. Any SN Ia model that has two narrow features in the B-peak $u-v$ color separated by more the 0.25 mag does not agree well with the data. Adding additional color smearing to the Milne-like model would make it agree better with the data, but would be inconsistent with the narrow widths of the color peaks seen in Milne et al. (2015).

5 CONCLUSIONS

Our analysis of the SDSS and SNLS supernova surveys does not agree with the observations reported in Milne et al. (2015). We do not observe two distinct red and blue samples in the rest frame near ultraviolet brightness of SN Ia at B-peak. Rather, we see a broad distribution well described by a combination of SN Ia color variations and extinction as given by the SALT-II model with a data derived distribution of its parameters, the SK16 model. Our simulations of the two surveys show that we can distinguish between the two $u-v$ color models, and our analysis of 158 light curves, specifically the 99 from the SNLS, show no evidence for the distinct $u-v$ peaks reported in Milne et al. (2015).

ACKNOWLEDGMENTS

We thank Peter Milne and Ryan Foley for useful discussions about their work. This work was supported in part by the Kavli Institute for Cosmological Physics at the University of Chicago through grant NSF PHY-1125897 and an endowment from the Kavli Foundation and its founder Fred Kavli.

R.K and D.S, gratefully acknowledges support from NASA grant 14-WPS14-0048. D.S. is supported by NASA through Hubble Fellowship grant HST-HF2-51383.001 awarded by the Space Telescope Science Institute, which is operated by the Association of Universities for Research in Astronomy, Inc., for NASA, under contract NAS 5-26555.

REFERENCES

Astier P., et al., 2006, Astronomy and Astrophysics, 447
Betoule M., et al., 2014, Astronomy and Astrophysics, 568
Breeveld A. A., Landsman W., Holland S. T., Roming P., Kuina N. P. M., Pagea M. J., 2011, AIP Conference Proceedings, 1358
Frieman J. A., et al., 2008, The Astronomical Journal, 135
Guy J., et al., 2010, Astronomy and Astrophysics, 523
Kessler R., et al., 2009, Publications of the Astronomical Society of Pacific, 121
Kessler R., et al., 2013, The Astrophysical Journal, 764
Milne P. A., 2016, Private communication with Peter Milne
Milne P. A., Foley R. J., Brown P. J., Narayan G., 2015, The Astrophysical Journal, 803
Olive K. A., et al., 2014, Chin. Phys., C38, 090001
Perlmutter S., et al., 1999, The Astrophysical Journal, 517
Riess A. G., et al., 1998, The Astronomical Journal, 116
Roming P. W. A., et al., 2005, Space Science Reviews, 120
Schlegel D. J., Finkbeiner D. P., Davis M., 1998, The Astrophysical Journal, 500
Scolnic D., Kessler R., 2016, The Astrophysical Journal Letters, 822
Scolnic D., et al., 2014, The Astrophysical Journal, 795, 45

6 APPENDIX

The list of the SNe Ia used in this analysis.

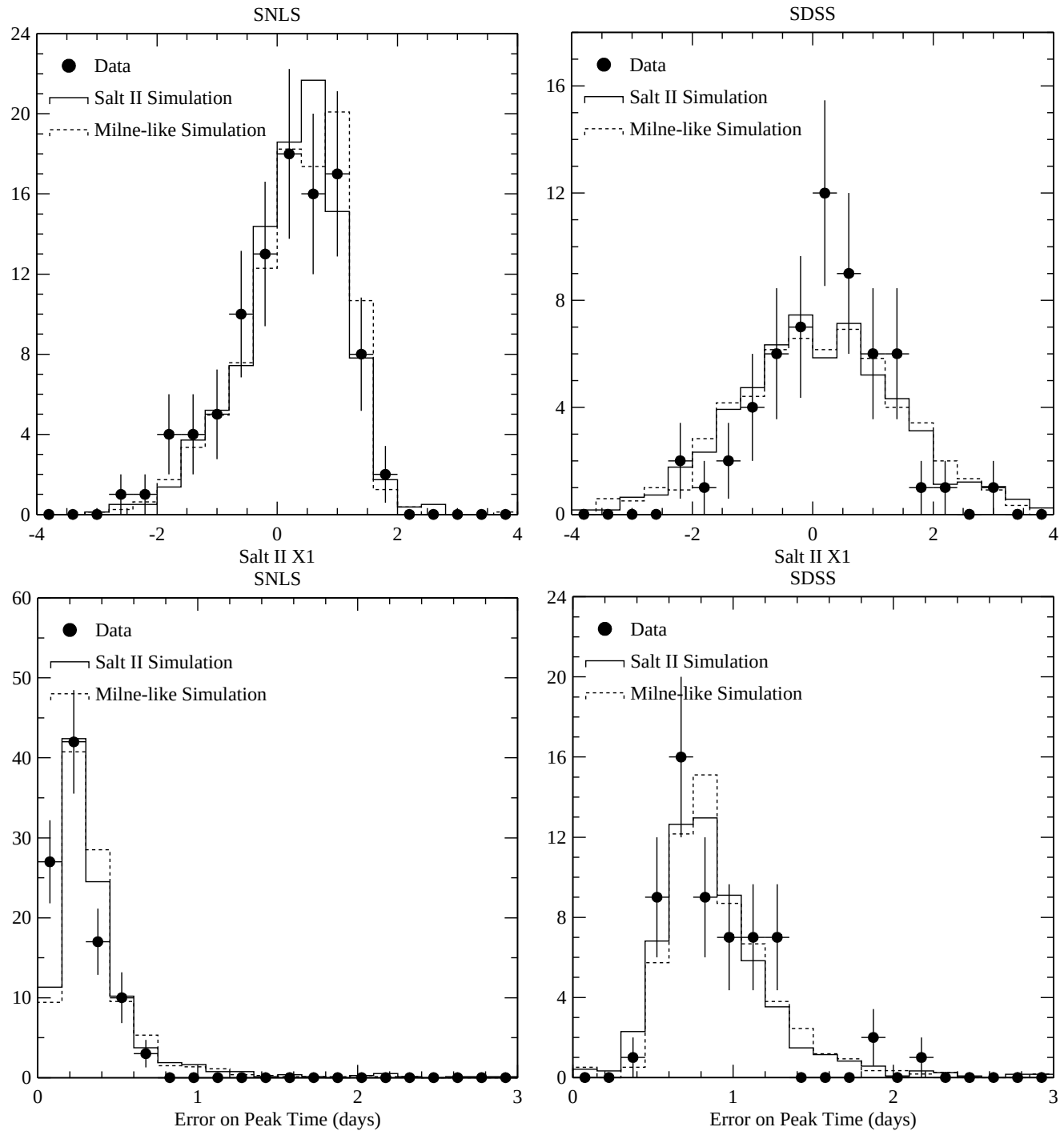

Figure 6. The distributions of the fitted values of the SALT-II x_1, stretch, parameter (top) and the uncertainty on the time of the B-peak (bottom) comparing the data and simulations of the SK16 and Milne-like models as described in the text in the SNLS (left) and SDSS (right) surveys.

The SNLS ID: 03D1au; 03D1aw; 03D1fc; 03D4au; 03D4cz; 03D4dh; 03D4dy; 03D4gf; 03D4gg; 04D1hd; 04D1hx; 04D1jg; 04D1kj; 04D1oh; 04D1pg; 04D1rh; 04D1sa; 04D2an; 04D2fp; 04D2fs; 04D2gb; 04D2gc; 04D2iu; 04D2mc; 04D2mh; 04D2mj; 04D3co; 04D3df; 04D3do; 04D3fk; 04D3kr; 04D3nh; 04D4an; 04D4bq; 04D4fx; 04D4gg; 04D4ib; 04D4ic; 04D4in; 04D4jr; 04D4ju; 05D1cc; 05D1ck; 05D1dn; 05D1dx; 05D1ee; 05D1hm; 05D1ix; 05D1ke; 05D1kl; 05D2ab; 05D2bv; 05D2cb; 05D2ci; 05D2ck; 05D2dt; 05D2dw; 05D2eb; 05D2hc; 05D2he; 05D2ie; 05D2le; 05D2mp; 05D3cf; 05D3ci; 05D3dd; 05D3gp; 05D3jq; 05D3jr; 05D3lb; 05D3lc; 05D3mh; 05D3mx; 05D4af; 05D4av; 05D4bf; 05D4bm; 05D4cw; 05D4dt; 05D4ef; 05D4ej; 05D4ek; 05D4ff; 05D4fo; 06D2bk; 06D2ca; 06D2cc; 06D2ck; 06D3cc; 06D3el; 06D3et; 06D2gb; 06D3df; 06D3ed; 06D3em; 06D4ba; 06D4bo; 06D4co; and 06D4cq.

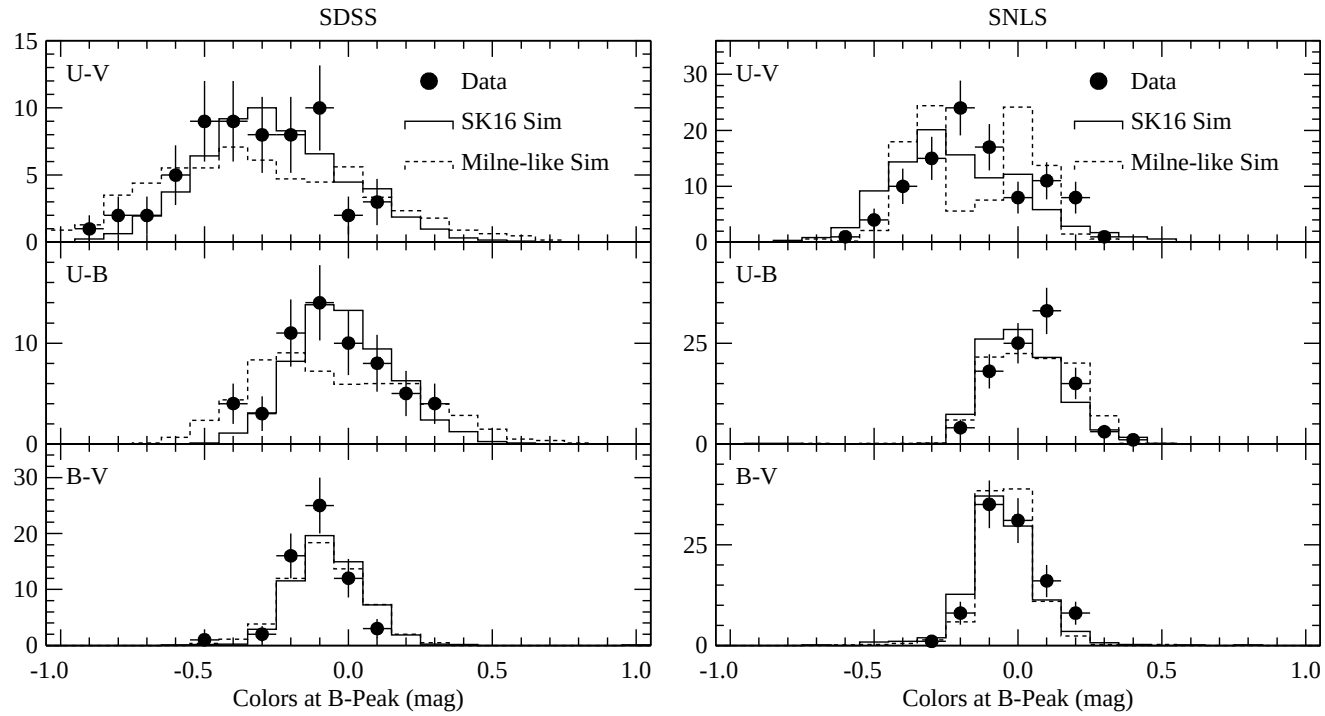

Figure 7. The fitted rest frame *B*-peak colors comparing the data and simulations of the SK16 and Milne-like models in the SDSS (left) and SNLS (right) surveys.

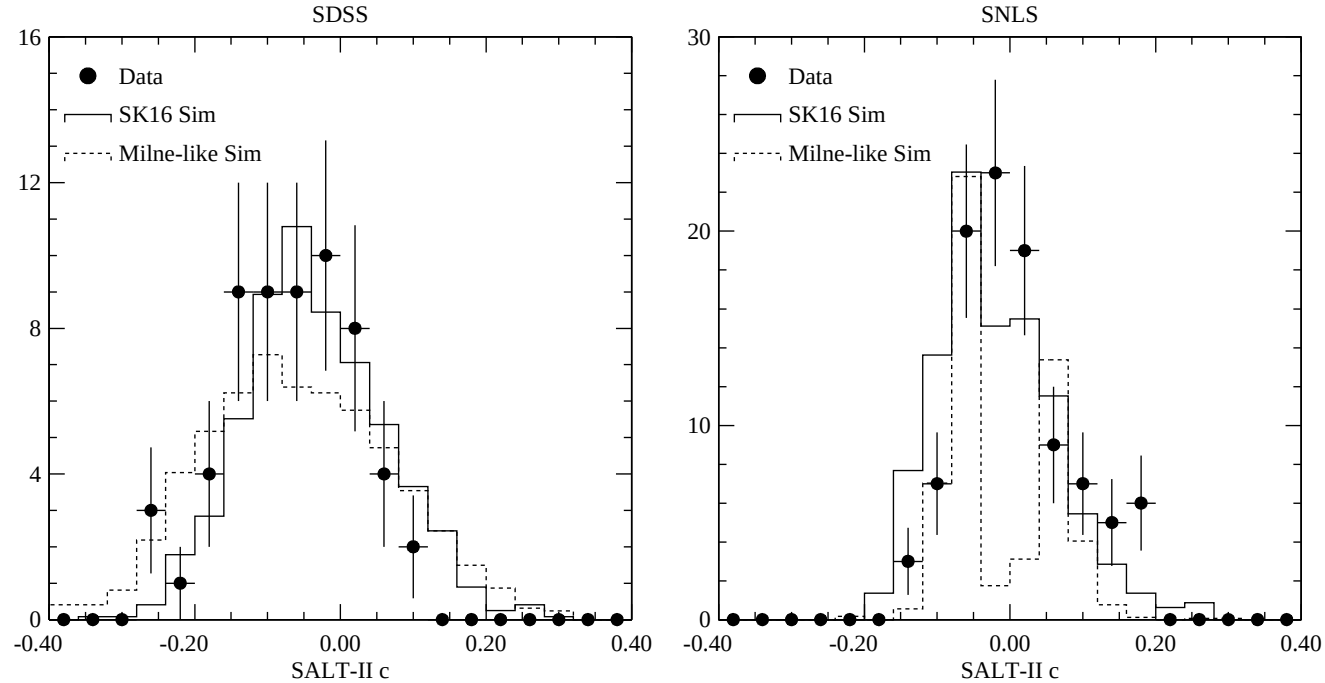

Figure 8. The fitted SALT-II color parameter comparing the data and simulations of the SK16 and Milne-like models in the SDSS (left) and SNLS (right) surveys.

The SDSS CID: 1166; 1688; 2533; 4241; 4679; 5183; 5391; 5737; 5844; 5966; 6100; 6137; 6649; 6699; 6924; 7143; 7475; 7779; 8598; 9045; 9207; 10550; 12883; 13136; 13830; 13934; 14397; 14456; 14735; 15170; 15213; 15217; 15383; 15456; 15704; 15756; 15776; 16000; 16093; 16211; 16232; 16421; 16779; 16789; 17528; 18091; 18617; 18782; 19029; 19033; 19632; 19818; 20106; 20142; 20184; 20186; 20245; 20432; and 21042.

This paper has been typeset from a TEX/LATEX file prepared by the author.